EARTHQUAKE ENGINEERING AND STRUCTURAL DYNAMICS
Earthquake Engng Struct. Dyn. 2008; **37**:975–990
Published online 17 March 2008 in Wiley InterScience (www.interscience.wiley.com). DOI: 10.1002/eqe.802

Estimation of hysteretic energy demand using concepts of modal pushover analysis

Tholen Prasanth[1,‡], Siddhartha Ghosh[1,*,†,§] and Kevin R. Collins[2,§]

[1]*Department of Civil Engineering, Indian Institute of Technology Bombay, Powai, Mumbai 400076, India*
[2]*Department of Civil Engineering, Lawrence Technological University, 21000 West Ten Mile Road, Southfield, MI 48075, U.S.A.*

SUMMARY

Hysteretic energy dissipation in a structure during an earthquake is the key factor, besides maximum displacement, related to the amount of damage in it. This energy demand can be accurately computed only through a nonlinear time-history analysis of the structure subjected to a specific earthquake ground acceleration. However, for multi-story structures, which are usually modeled as multi-degree of freedom (MDOF) systems, this analysis becomes computation intensive and time consuming and is not suitable for adopting in seismic design guidelines. An alternative method of estimating hysteretic energy demand on MDOF systems is presented here. The proposed method uses multiple 'generalized' or 'equivalent' single degree of freedom (ESDOF) systems to estimate hysteretic energy demand on an MDOF system within the context of a 'modal pushover analysis'. This is a modified version of a previous procedure using a single ESDOF system. Efficiency of the proposed procedure is tested by comparing energy demands based on this method with results from nonlinear dynamic analyses of MDOF systems, as well as estimates based on the previous method, for several ground motion scenarios. Three steel moment frame structures, of 3-, 9-, and 20-story configurations, are selected for this comparison. Bias statistics that show the effectiveness of the proposed method are presented. In addition to being less demanding on the computation time and complexity, the proposed method is also suitable for adopting in design guidelines, as it can use response spectra for hysteretic energy demand estimation.

Received 31 May 2007; Revised 13 December 2007; Accepted 23 January 2008

KEY WORDS: seismic damage; nonlinear dynamic analysis; hysteretic energy demand; modal pushover analysis; energy-based seismic design

*Correspondence to: Siddhartha Ghosh, Department of Civil Engineering, Indian Institute of Technology Bombay, Powai, Mumbai 400076, India.
†E-mail: sghosh@civil.iitb.ac.in
‡Former Graduate Student.
§Assistant Professor.

1. INTRODUCTION

The current seismic design state-of-the-practice throughout the world is the elastic-force-based design approach using acceleration spectra. Over the past few decades, there has been a significant effort from the earthquake engineering research community to move towards a more rational approach to design through better characterization of the damage potential. This resulted in displacement-based considerations being included in the prospective design approaches of the new millennium. However, many researchers identified hysteretic energy demand or its equivalent parameters as the demand parameters, which are most closely correlated to seismic damage of structures [1–3]. Hysteretic energy is the energy that is dissipated through the inelastic deformations in a structure at various cyclic load reversals. Unlike other demand parameters, such as yield base shear or inelastic story drift, the hysteretic energy demand takes into account the effects of the duration of the earthquake and the cyclic-plastic deformation behavior of the structure. A design approach based on hysteretic energy demand, thus, has the potential to account for the damage potential explicitly.

An attempt to define an energy-based design procedure was made by Housner as early as 1956 [4]. Although various researchers stressed the necessity of an energy-based design methodology [1, 2, 5] and the important role it would play in the advanced seismic codes of the future, it did not gain significant recognition as one of the prospective design procedures until the publication of the Vision 2000 document [6]. This document proposed, for advanced seismic design guidelines of the future, the comprehensive design, the displacement-based design, and the energy-based design approaches as potential design approaches needing development.

Estimation of hysteretic energy demand on real structures is one of the major aspects of developing energy-based design methods. This was highlighted by some recent studies on energy-based design and on seismic energy demand [3, 7–10]. With the computing facilities available today, the estimation of hysteretic energy demand for a specific structure under a certain earthquake ground motion is not difficult, although it is computation intensive. However, one has to apply this detailed method (nonlinear response-history analysis of a multi-degree of freedom (MDOF) model) for each individual structure separately, which makes this method unsuitable for incorporating in a general purpose design methodology based on hysteretic energy demand. Similar problems in force- or displacement-based design approaches were solved by the use of response spectra and 'equivalent' or 'generalized' single degree of freedom (SDOF) models of a structure. Ghosh and Collins [9] applied this concept in exploring the possibility of a hysteretic energy-based design methodology. They developed hysteretic energy response spectra based on the demand on an inelastic SDOF system. A structure-specific equivalent single degree of freedom (ESDOF) system was developed based on a pushover analysis of the actual MDOF system. Using simple scaling relationships, the hysteretic energy response spectra ordinates were converted to values for the ESDOF model of the real structure. However, as those results showed, there were considerable differences between the actual demands (based on the MDOF model) and the estimated demands (based on the ESDOF model) for several cases. Those discrepancies provided the motivation for the work presented herein.

Similar drawbacks in the traditional nonlinear pushover analysis in estimating the dynamic displacement demand prompted researchers to develop advanced pushover analysis techniques, such as the 'modal' or 'adaptive' pushover analysis [11, 12]. These new procedures used several ESDOF systems, instead of a single ESDOF system, for estimating the response of a structure. The multiple ESDOF systems were obtained from various pushover analyses of the structure, and

DOI: 10.1002/eqe

these pushover analyses utilized the dynamic (modal) properties of the system. The results showed improvement over estimations based on traditional pushover techniques.

The present article proposes a multiple equivalent systems-based approach, using a concept similar to the modal pushover analysis (MPA), for estimating hysteretic energy demand on a structure. The following two sections provide further details on the previous energy-based method proposed by Ghosh and Collins [9] and on the modal pushover technique, respectively. The proposed method is presented in the fourth section, followed by case studies for three steel moment frame structures (3-, 9-, and 20-story) under various ground motion scenarios.

2. ESTIMATING HYSTERETIC ENERGY DEMAND USING A SINGLE EQUIVALENT SYSTEM

The concept of an equivalent SDOF model of an MDOF system is not new. An ESDOF system is a simplistic representation of an actual MDOF structure, such that the ESDOF system is capable of representing certain response(s) of the MDOF structure. Ghosh and Collins [9] developed an ESDOF approach for estimating hysteretic energy demand of real MDOF structures. The formulation of a generalized or equivalent system starts from the dynamic response of a two-dimensional MDOF cantilever-type structure subjected to horizontal base motion:

$$\mathbf{m}\ddot{\mathbf{u}}+\mathbf{c}\dot{\mathbf{u}}+\mathbf{r}=-\mathbf{m}\mathbf{1}\ddot{u}_g \tag{1}$$

where $\mathbf{m}$ is the mass matrix, $\mathbf{c}$ is the damping matrix, $\mathbf{u}$ is the lateral displacement vector, and $\mathbf{r}$ is the restoring force vector. Assuming a time-invariant deformation shape vector $\boldsymbol{\phi}$, normalized to have a value of 1 corresponding to roof displacement, Ghosh and Collins reduced the MDOF model to an ESDOF system with the following equation of motion [9]

$$\ddot{q}+2\xi\omega\dot{q}+\omega^2 G(q)=-\Gamma\ddot{u}_g \tag{2}$$

where $\Gamma=L/M$, $M=\boldsymbol{\phi}^{\mathrm{T}}\mathbf{m}\boldsymbol{\phi}$, $L=\boldsymbol{\phi}^{\mathrm{T}}\mathbf{m}\mathbf{1}$, $2\xi\omega=C/M$, $C=\boldsymbol{\phi}^{\mathrm{T}}\mathbf{c}\boldsymbol{\phi}$, $\omega^2=K/M$, and $K=K_{\mathrm{po}}\boldsymbol{\phi}^{\mathrm{T}}\mathbf{f}$. The detailed derivation of Equation (2) from Equation (1) is presented in an earlier report by Ghosh [13]. $G(q)$ is a function representing the force–displacement behavior of the ESDOF system. This function is obtained from a nonlinear pushover analysis of the MDOF structure. The vector $\mathbf{f}$ represents the normalized lateral force distribution assumed in the pushover analysis as per UBC-97 [14]. This vector is normalized to achieve a unit base shear ($V=1$). A bilinear approximation of the pushover curve (base shear *vs* roof displacement plot) provides the elastic stiffness K_{po}, the yield (roof) displacement D_{y}, and the strain hardening stiffness ratio α_k. These parameters are obtained using an approximation similar to the one shown in Figure 1. The shape vector $\boldsymbol{\phi}$ is based on the displaced shape at 1% global drift obtained from the pushover analysis. The details regarding obtaining these parameters from pushover analysis were provided in previous works [9, 13].

Ghosh and Collins [9] used Equation (2) to obtain hysteretic energy demands using ESDOF idealizations for different symmetric-in-plan building structures, under various earthquake scenarios. These were the 3-, 9-, and 20-story SAC Steel buildings in Los Angeles, U.S.A. [11], which follow the standard strong column-weak beam design as per UBC-94 [15], and were considered for many analytical works in the recent past. These results were compared with those from Equation (1)

DOI: 10.1002/eqe

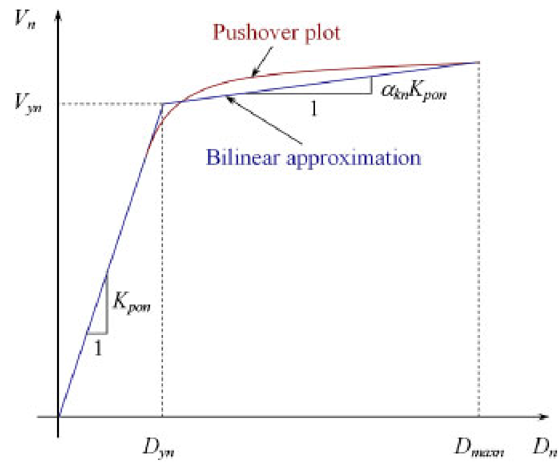

Figure 1. Bilinear approximation of the pushover ($V_n - D_n$) curve.

using the MDOF system modeling of the same buildings. This equivalent system approach was able to estimate the hysteretic energy demand for the low-rise (3-story) building with sufficient accuracy (with an average error of 25%) [9]. However, the degree of accuracy decreased when it was applied to the 9-story building, and it decreased further for the 20-story building. Nevertheless, the convenience of this approach remains that it can be incorporated in a design method because it can utilize a response spectrum for demand estimation. The results from these analyses are presented later along with the results from the newly developed procedure.

3. MODAL PUSHOVER ANALYSIS

The limitation of the traditional pushover procedure is that it cannot effectively account for the contribution of higher modes in the estimation of seismic demands. In the MPA procedure proposed by Chopra and Goel [11, 12], this limitation was overcome by using multiple ESDOF systems based on more than one mode of vibration. These ESDOF systems were obtained from nonlinear static pushover analyses corresponding to elastic vibration modes of the MDOF system. The MPA was used for estimating seismic demands of nonlinear (inelastic) as well as linear elastic MDOF systems with sufficient closeness to results obtained from a response-history analysis. The advantage of MPA is that it achieves this degree of accuracy without losing the conceptual simplicity and computational attractiveness of the traditional pushover procedure.

The parameters of an ESDOF system corresponding to the nth mode of vibration of the MDOF model were calculated by conducting a nonlinear static pushover analysis of the structure with a lateral force distribution proportional to $\mathbf{f}_n = \mathbf{m}\boldsymbol{\phi}_n$, where $\boldsymbol{\phi}_n$ is the nth mode shape. The governing equation of motion for the nth mode inelastic ESDOF system was expressed as

$$\ddot{q}_n + 2\xi_n \omega_n \dot{q}_n + \frac{F_{sn}}{M_n} = -\Gamma_n \ddot{u}_g \tag{3}$$

DOI: 10.1002/eqe

where the resisting force quantity F_{sn} is a function of the modal coordinate q_n. The relationship between the resisting (elastic or inelastic) force parameter F_{sn}/M_n and the modal coordinate q_n of the nonlinear ESDOF system was estimated from an idealized V_n (base shear) *vs* D_n (roof displacement) pushover curve of the nth mode, where

$$F_{sn} = \frac{V_n}{\Gamma_n} \quad \text{and} \quad q_n = \frac{D_n}{\phi_{rn}} \tag{4}$$

Here ϕ_{rn} is the value in the shape vector $\boldsymbol{\phi}_n$ corresponding to the roof displacement. Equation (3) can be solved conveniently to obtain the displacement time history. Alternatively, the peak value of $q_n(t)$ can also be estimated using an inelastic response spectrum. The peak inelastic response of the MDOF system was estimated by combining (by using appropriate modal combination rules, such as SRSS or CQC) the peak inelastic responses of the ESDOF systems corresponding to the first few modes [11].

It should be noted here that Equations (2) and (3) come from the same idealization and they both express the same inelastic dynamic phenomenon of a generalized coordinate. The primary differences, other than the use of modal properties in MPA, are that:

1. The influence vector used in MPA is a more general influence vector $\boldsymbol{\iota}$ [11], instead of a unit vector that is used for regular building structures modeled with only horizontal displacement degrees of freedom.
2. The shape vector $\boldsymbol{\phi}$ does not need to be normalized for the MPA procedure, contrary to the normalization to 1 for roof displacement for the method proposed by Ghosh and Collins [9].
3. The MPA procedure uses a specific definition of lateral force vector $\mathbf{f} = \mathbf{m}\boldsymbol{\phi}$. The procedure by Ghosh and Collins [9] allows $\mathbf{f}$ to be defined more generally.

The MPA was applied effectively to obtain inelastic force and displacement demands in three symmetrical-plan steel moment frame buildings (3-, 9-, and 20-story SAC Steel buildings in Los Angeles, U.S.A.) [11]. The MPA was later extended to the estimation of seismic demands in unsymmetrical-plan buildings as well [12].

4. ESTIMATION OF HYSTERETIC ENERGY DEMAND USING MULTIPLE EQUIVALENT SYSTEMS

The equivalent system approach, proposed by Ghosh and Collins [9], was not effective in estimating the hysteretic energy demand for taller buildings, although it was effective for a low-rise building. This method seems to suffer from the same limitation as the traditional pushover analysis of not being able to account for the higher mode effects. A multiple equivalent systems approach similar to the MPA, where contributions from various modes are incorporated, should be able to estimate hysteretic energy demand for high-rise structures as well. A two ESDOF systems-based similar approach was used by Chou [16] and Chou and Uang [17] to estimate absorbed energy (elastic energy plus hysteretic energy) demand. This method used earthquake-specific constant-ductility equivalent velocity spectra for obtaining the absorbed energy demand, where the ductility demand for each modal equivalent ESDOF system is obtained from inelastic C_{y} response spectra.

DOI: 10.1002/eqe

This method was used successfully to estimate the absorbed energy demand for several low- to mid-rise (3-, 5-, 7-, and 9-story) steel-framed structures under two to three earthquake scenarios.

For the proposed method of estimating hysteretic energy demand, Equation (2) is rewritten using modal terminology and notation. For the ESDOF system corresponding to the nth mode shape $\boldsymbol{\phi}_n$:

$$\ddot{q}_n + 2\xi_n \omega_n \dot{q}_n + \omega_n^2 G_n(q_n) = -\Gamma_n \ddot{u}_g \tag{5}$$

However, here the lateral force distribution $\mathbf{f}_n$ for pushover analysis is obtained based on the nth mode shape (instead of the UBC-recommended lateral force distribution), after normalizing $\mathbf{m}\boldsymbol{\phi}_n$ to a unit base shear ($\mathbf{f}_n = \mathbf{m}\boldsymbol{\phi}_n / \boldsymbol{\iota}^{\mathrm{T}}\mathbf{m}\boldsymbol{\phi}_n$). Note that the vector $\boldsymbol{\phi}_n$ is normalized in the same way as it was done for the shape vector $\boldsymbol{\phi}$ by Ghosh and Collins [9], that is, $\phi_{rn} = 1$.

For each mode, the pushover analysis is carried out to a maximum interstory drift of 2.5%. Here, the maximum interstory drift is selected as the limiting value, instead of the global drift, because for higher modes limiting the global drift may not necessarily limit the story drifts to realistic values and that may lead to instability. There is no specific justification for using a 2.5% drift limit. As shown in a previous report [13], using other drift limits for the bilinear approximation does not have any significant effect on the equivalent system parameters. The base shear V_n *vs* roof displacement D_n 'pushover' curve is approximated by a bilinear function by equating the areas underneath the curves (Figure 1). The bilinear curve gives the elastic stiffness $K_{\mathrm{po}n}$, the yield displacement $D_{\mathrm{y}n}$ $(= V_{\mathrm{y}n}/K_{\mathrm{po}n})$, and the strain hardening stiffness ratio α_{kn} from which the critical parameters for the nth mode equivalent system are obtained, similarly as in Ghosh and Collins' procedure [9]. The participation factor for each mode is obtained as

$$\Gamma_n = \frac{\boldsymbol{\phi}_n^{\mathrm{T}}\mathbf{m}\boldsymbol{\iota}}{\boldsymbol{\phi}_n^{\mathrm{T}}\mathbf{m}\boldsymbol{\phi}_n} \tag{6}$$

The hysteretic energy demand in each mode E_{nh} is obtained by solving the nonlinear dynamic relation of Equation (5). Since E_{nh} is a cumulative (non-decreasing) function in time, the peak hysteretic energy will always occur at the end of the analysis. A simple way to combine the individual E_{nh} values is to add them together. However, this is still an approximation because it ignores any coupling in the inelastic domain that may occur [11].

The following section describes how this approach of estimating hysteretic energy demand using multiple ESDOF systems is applied for the same three SAC steel buildings under various ground motion scenarios.

5. THREE TEST CASES FOR THE PROPOSED PROCEDURE

5.1. Description of the test structures

The proposed procedure is tested for three steel moment frame buildings under various ground motion scenarios. They are the three 'pre-Northridge' designs of 3-, 9-, and 20-story buildings in Los Angeles, U.S.A. (considered in the SAC Steel Project) studied by Chopra and Goel [11] and Ghosh and Collins [9]. These structures meet the seismic code requirements as per UBC-94 [15] and represent typical low-, medium-, and high-rise buildings designed for Los Angeles at that time. The primary reason for selecting these buildings for test cases is that the results can be compared with the results obtained using the method proposed by Ghosh and Collins [9]. Details

DOI: 10.1002/eqe

regarding frame dimensions, material properties, and loads can be obtained from previous research works [18].

For each building, a two-dimensional model of the North–South moment frame representing the building is considered. This frame is modeled for nonlinear static and dynamic analyses in DRAIN-2DX [19], based on its centerline dimensions. A simple bilinear inelastic beam-column element with no strain hardening is used for modeling beams and columns. The joint panel zones are assumed to be rigid. The stiffness contribution of the gravity frames (interior frames) is not considered. Effects of gravity loads and the P-Delta effects are also neglected to keep the test cases simple. Damping ratios of 5% are assumed for the first two modes.

5.2. Estimation of hysteretic energy demand

Following is a stepwise description of the calculation of hysteretic energy demand using multiple ESDOF systems:

1. The mode shape vectors $\boldsymbol{\phi}_n$ are obtained from an eigenvalue analysis of the elastic two-dimensional frame model. For example, Figure 2 illustrates the first three elastic mode shapes for the 9-story building, normalized to a unit roof displacement. The generalized mass M_n and modal participation factor Γ_n for each mode are also calculated based on these mode shapes.
2. Nonlinear pushover analysis is carried out for each mode with a normalized lateral force distribution of $\mathbf{f}_n$, until the maximum inter-story drift reaches 2.5%. Figure 3 shows such lateral force distributions that are used for pushover analysis for the first three modes of the 9-story frame.
3. The pushover curve for each mode is approximated by a bilinear curve, and force-deformation parameters (K_{pon}, D_{yn}, and α_{kn}) are obtained from this approximation. The stiffness parameter of the nth mode ESDOF system is calculated as $K_n = K_{\text{pon}} \boldsymbol{\phi}_n^{\text{T}} \mathbf{f}_n$. For example, Table I

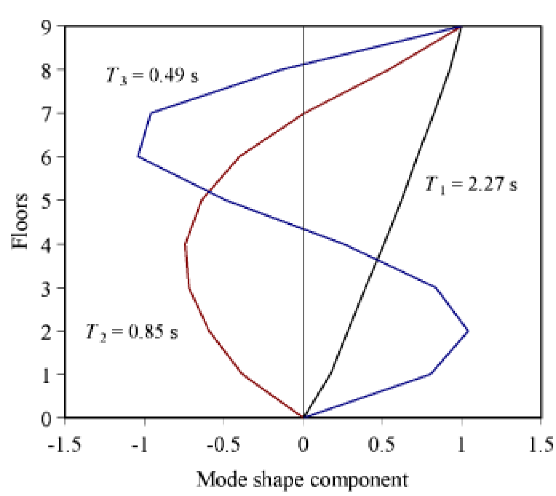

Figure 2. Elastic mode shapes ($\boldsymbol{\phi}_n$) for the first three modes ($n = 1$–3) for the 9-story frame.

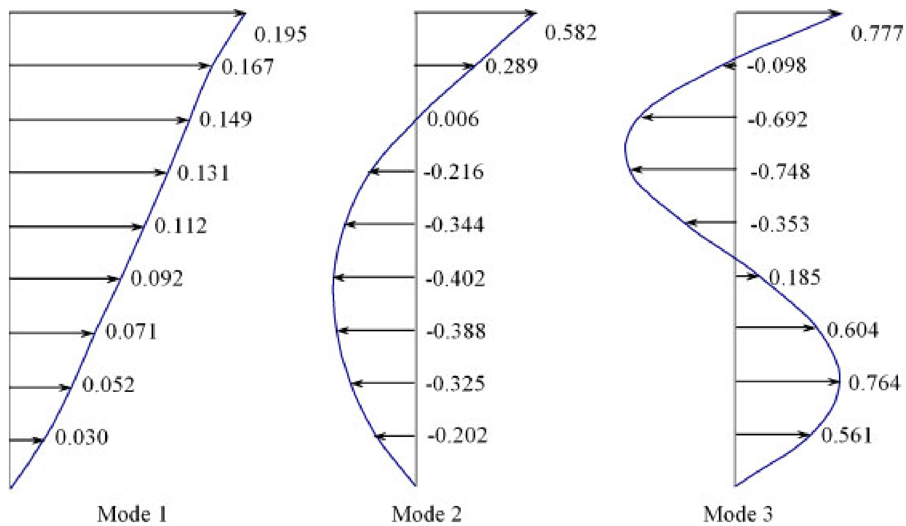

Figure 3. Normalized lateral load distributions $\mathbf{f}_n$ for the first three modes ($n=1$–3) for the 9-story frame.

Table I. ESDOF parameters corresponding to the first five modes of the 9-story building.

Mode	T_n (s)	M_n (kN s^2/m)	Γ_n	K_n (10^3 kN/m)	α_{kn}
1	2.27	2004	1.366	15.39	0.188
2	0.85	1734	0.529	94.21	0.075
3	0.49	2884	0.238	471.2	0.037
4	0.33	4133	0.113	1476	0.013
5	0.22	7436	0.053	5950	0.002

shows the required parameters for ESDOF systems corresponding to the first five modes for the 9-story building. Each ESDOF system is assumed to have 5% damping.

4. Hysteretic energy demands (E_{nh}) for ESDOF systems, corresponding to the first five modes, are obtained using nonlinear time-history analyses. These analyses are carried out for each building for 10 real and 8 simulated earthquake scenarios. These are the same earthquakes for which Ghosh and Collins' method was tested. For detailed information on these ground acceleration data, refer to the previous report by Ghosh [13].
5. For each earthquake, the E_{nh} values for the first five modes are added to obtain the estimate of hysteretic energy demand on a structure. This total is denoted as E_{MPA}.

To evaluate how well the MPA-based procedure works in predicting energy demands, a bias factor is defined as

$$N_{\mathrm{MPA}} = \frac{E_{\mathrm{NL\text{-}RHA}}}{E_{\mathrm{MPA}}} \tag{7}$$

DOI: 10.1002/eqe

where $E_{\text{NL-RHA}}$ is the hysteretic energy demand based on the nonlinear response-history analysis of the MDOF model of the actual structure. This bias factor is calculated for each earthquake and provides a quick way to evaluate how much the MPA procedure overpredicts or underpredicts demands. Table II provides the bias statistics for the three buildings for all 18 earthquakes considered.

Table II also provides comparison, in terms of the bias factor, between the proposed MPA procedure and the previous one [9] using a single ESDOF system. The hysteretic energy estimated using the previous procedure is labeled as E_{UBC}, since it used an equivalent system based on the UBC-recommended pushover analysis. The bias for the previous procedure (N_{UBC}) is defined similarly as in Equation (7) with E_{MPA} replaced by E_{UBC}. The 'UBC' procedure yielded very unrealistic estimates for four records for the 20-story building, which are marked with †. The average, standard deviation, and coefficient of variation for each column are shown at the bottom of the table. In addition, simple scatterplots (Figure 4) are also provided here for an easy comparison between the two procedures. A scatterplot provides comparison for all the earthquakes considered for a selected structure. The diagonal line across a scatterplot represents perfect agreement between the nonlinear response history analysis and the approximate analysis technique.

Table II. Bias factor statistics for the three buildings for the MODAL and the UBC procedures.

	Bias factor					
	3-Story		9-Story		20-Story	
Ground motion record*	N_{UBC}	N_{MPA}	N_{UBC}	N_{MPA}	N_{UBC}	N_{MPA}
s640r005	1.09	1.12	1.91	1.19	3.75	1.82
s503r005	1.37	1.13	2.44	1.36	1.65	1.10
s065r005	1.31	1.07	1.55	1.32	2.34	1.41
s621r004	1.35	1.18	1.18	1.04	5.14	1.14
s050r005	1.01	1.01	1.15	1.01	1.14	1.13
s212r008	1.21	1.08	1.44	1.15	1.07	1.12
s305r008	1.09	1.02	1.23	1.00	1.91	1.10
s549r009	1.05	1.03	1.16	0.98	0.97	1.04
nr	1.08	1.08	1.46	0.99	3.21	1.10
ns	0.97	0.95	2.01	1.20	†	1.51
chy08036	1.07	1.06	4.45	1.17	†	2.39
chy0809	1.08	1.05	2.77	1.11	†	1.30
tcu0659	1.01	1.00	1.30	1.14	1.01	0.98
syl90	1.48	1.12	1.15	1.01	†	2.05
newh360	1.06	1.04	2.11	1.39	2.95	1.30
nh	1.25	1.11	1.01	0.92	4.80	1.13
syl360	1.26	1.12	1.01	0.95	4.03	1.19
tcu06536	1.05	1.03	1.27	1.20	1.93	1.82
Mean	1.16	1.07	1.70	1.12	2.56	1.37
SD	0.147	0.056	0.853	0.142	1.43	0.397
CoV	0.127	0.053	0.502	0.127	0.559	0.290

*Information regarding these records can be found in the report by Ghosh [13].

†These records are not used for calculating bias statistics for the UBC procedure for the 20-story building as it yields very unrealistic estimates.

DOI: 10.1002/eqe

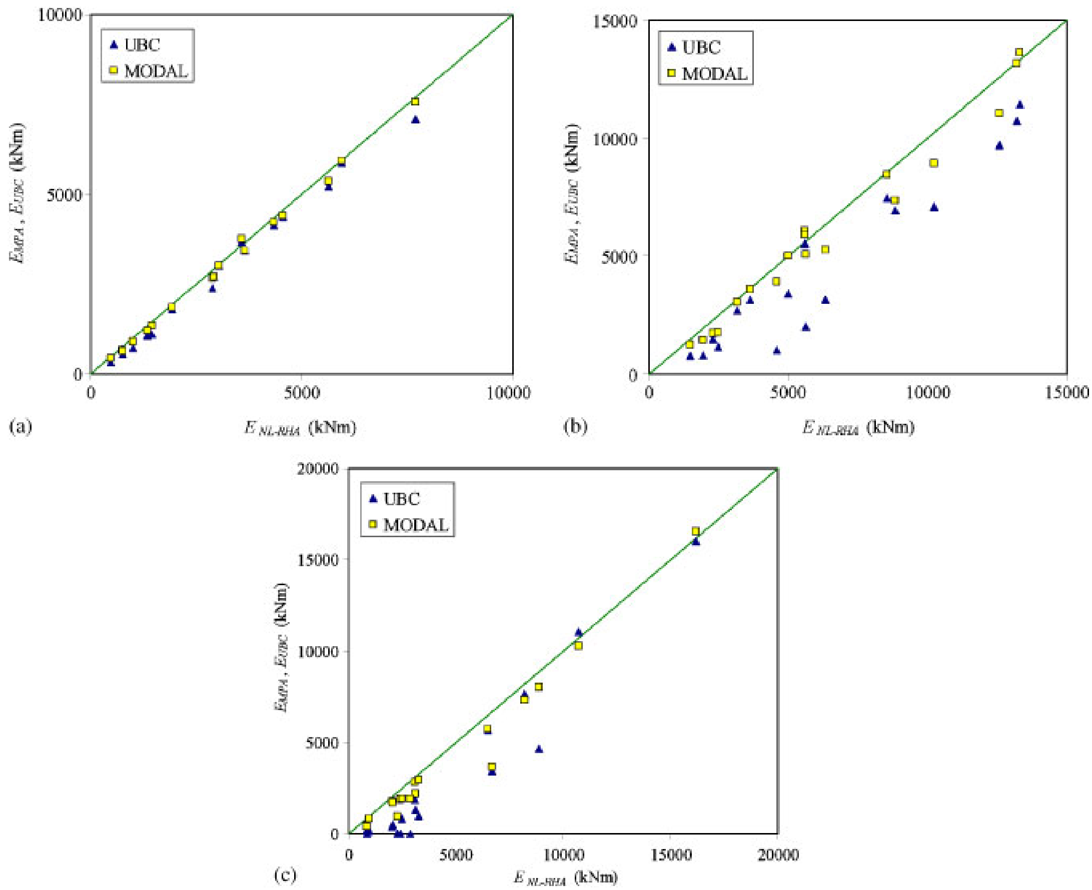

Figure 4. Scatterplots comparing E_{MPA} and E_{UBC} with $E_{\text{NL-RHA}}$ for the (a) 3-story, (b) 9-story, and (c) 20-story buildings.

6. INTERPRETATION OF RESULTS

Table II and the scatterplots in Figure 4 provide the outcomes of the three test cases. The averages and coefficients of variation clearly indicate that the proposed 'MODAL' procedure of estimating hysteretic energy demand provides more accurate (that is, closer to $E_{\text{NL-RHA}}$) estimates than the UBC procedure. The mean bias for the proposed method (N_{MPA}) is closer to its ideal value of 1.0 than the mean bias of the previous estimate (N_{UBC}) in all the three cases. The standard deviations and the coefficients of variation values are also less in each case compared with the previous method of estimation. The improvement is particularly significant for the cases of the 9- and the 20-story buildings. With few exceptions, this improvement is also evident when comparing results for each individual earthquake record.

The scatterplots in Figure 4 provide a quick and easy way to compare the two methods, and these also show very clearly the MODAL estimates to be closer to the ideal diagonal line, compared with the UBC estimates.

DOI: 10.1002/eqe

The E_{nh} values from each mode obtained in these analyses show that it is not the only fundamental mode that is contributing to the hysteretic energy demand on the actual structure. For example, a mode-wise distribution of hysteretic energy demand (E_{nh}) for the first five modes of the 20-story building is shown in Table III. These results show that considering only three modes for the 20-story building would give the same results. For many of the records, only the first mode contributes significantly. Observe, however, the interesting results for four of the records where the second and third mode contributions are significant. These results are unique because of the nature of the ground motion records. Two of these records ('chy08036' and 'chy0809') are records from the 1999 Chi-Chi earthquake in Taiwan. A reconnaissance report for this earthquake [20] documents some of the interesting characteristics of the ground motions from this event, such as the significant record-to-record variability and the high spectral accelerations at both short and long periods. Figure 5 provides a plot of the pseudo-acceleration response spectra for the two Chi-Chi records mentioned above and a third Chi-Chi record 'tcu0659'. To relate these plots to the results in Table III, note that the periods of the first three modes of the 20-story building are 3.81, 1.32, and 0.766 s. The spectral ordinates for records 'chy08036' and 'chy0809' are two to three times larger in value (than for the record 'tcu0659') in the vicinity of the third mode period and are also larger in the vicinity of the second mode period. However, they are lower near the first mode period. Of course, these response spectra are based on elastic response and not inelastic response, but they do provide some insight into why the contributions from the higher modes in Table III for the two Chi-Chi records seem unusually large.

It can be noted that for most of the selected earthquakes, only the first mode contributes significantly. Therefore, a modification of the single equivalent system-based method proposed by Ghosh and Collins [9], with elastic mode shape-based $\boldsymbol{\phi}$ and $\mathbf{f}$ vectors, will provide good estimates

Table III. Mode-wise distribution of hysteretic energy demands for the 20-story building.

	E_{nh}/E_{MPA} (where $E_{\text{MPA}}=\sum_{n=1}^{5} E_{nh}$)				
Ground motion record	Mode 1 (%)	Mode 2 (%)	Mode 3 (%)	Mode 4 (%)	Mode 5 (%)
s640r005	100	0	0	0	0
s503r005	100	0	0	0	0
s065r005	100	0	0	0	0
s621r004	100	0	0	0	0
s050r005	97.8	2.2	0	0	0
s212r008	100	0	0	0	0
s305r008	73.1	26.6	0.3	0	0
s549r009	98.0	2.0	0	0	0
nr	43.5	51.4	5.1	0	0
ns	30.9	67.7	1.4	0	0
chy08036	6.7	93.3	0	0	0
chy0809	0	79.7	20.3	0	0
tcu0659	98.1	1.9	0	0	0
syl90	100	0	0	0	0
newh360	69.4	30.6	0	0	0
nh	80.3	19.7	0	0	0
syl360	79.5	20.5	0	0	0
tcu06536	100	0	0	0	0

DOI: 10.1002/eqe

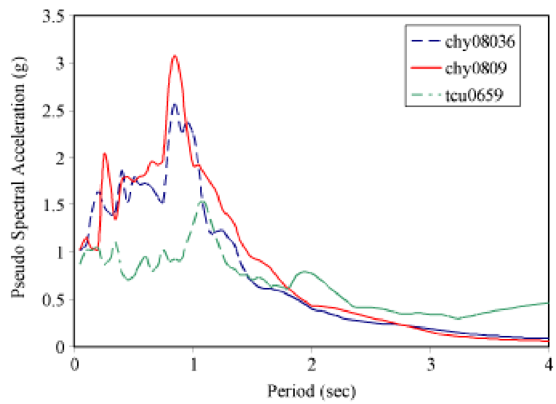

Figure 5. Pseudo-acceleration response spectra (for 5% damping) for three records from the 1999 Chi-Chi earthquake in Taiwan: ‘chy08036’, ‘chy0809’, and ‘tcu0659’.

of hysteretic energy demand for many, but not all, earthquakes. This statement applies only to regular, symmetric-plan buildings. Further investigations are needed for irregular buildings.

It can also be noted from the scatterplots as well as from Table II that E_{MPA} underestimates the actual response ($E_{\text{NL-RHA}}$) for most of the earthquake records considered, and the difference increases as the number of stories increases. This may be attributed to the coupling of higher modes in the inelastic domain. Such inelastic coupling cannot be properly accounted for through analyses of independent modal equivalent systems. The effect of concentrated inelastic activity in the top stories of a high-rise building frame, or the ‘whiplash’ effect [21], can also be the reason for a higher degree of underestimation of energy demand for such frames based on the proposed procedure. To check the possibility of a whiplash, the hysteretic energy demand on the top three stories of the 20-story frame is computed (using nonlinear response-history analysis) for three earthquake cases, in which we see a large bias (namely, ‘s065r005’, ‘chy08036’, and ‘tcu06536’). However, the hysteretic energy demands in the top three stories are observed to be only 0.56, 7.8, and 1.48% of the total hysteretic energy demand ($E_{\text{NL-RHA}}$), respectively, for these three earthquakes. Since these amounts do not account for the large bias factors (1.41, 2.39, and 1.82, respectively), the whiplash effect cannot be assigned as the primary reason for the underestimation.

7. COMPARISON WITH MODAL DISPLACEMENT DEMANDS

As reported in Section 3, previous researchers successfully applied MPA to obtain elastic and inelastic displacement demands in MDOF systems [11]. A comparison between the applications of modal pushover concepts for estimating hysteretic energy demands and displacement demands is provided in this section. For the same three test frames and the same set of earthquake records, MPA is applied to obtain the absolute maximum roof displacement (D). The accuracy of the method is tested through scatterplots (Figure 6) and bias factors (Table IV) as in the previous case. The peak modal demands are combined using both the SRSS and the ABSSUM rules [22].

It is observed that similar to the hysteretic energy estimates, the average difference between D_{MPA} and $D_{\text{NL-RHA}}$ increases as the number of story increases. However, unlike the energy

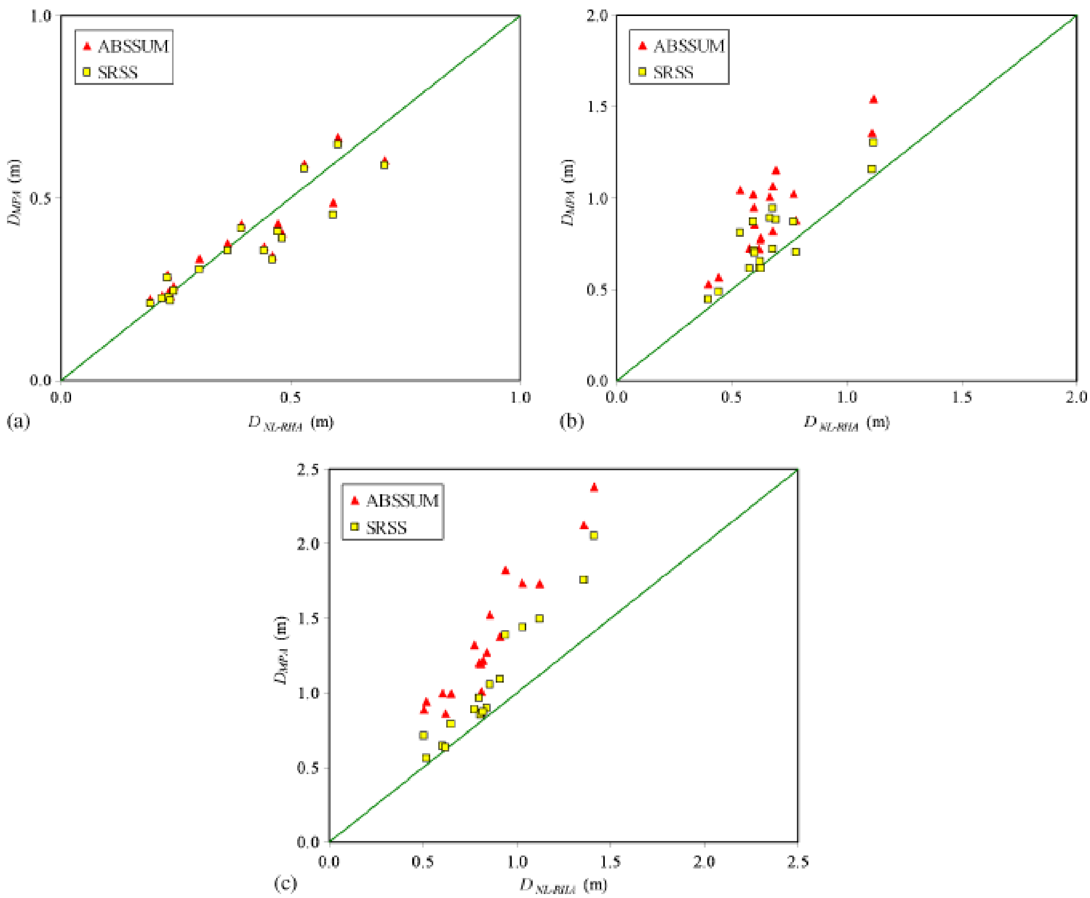

Figure 6. Scatterplots comparing D_{MPA} with $D_{\mathrm{NL\text{-}RHA}}$ for the (a) 3-story, (b) 9-story, and (c) 20-story buildings.

estimates, the modal method tends to overestimate the displacement demand in most earthquake cases, particularly for the 9- and 20-story buildings. The non-coherence of peak displacement responses for individual modes, which are combined using ABSSUM or SRSS, may be the primary reason for this overestimation in the majority of the cases.

Table V presents a mode-wise distribution of peak roof displacements (D_n) for the first five modes of the 20-story building, based on the ABSSUM combination rule. Since the displacement demand can be both elastic and inelastic, we see contributions from all the modes as opposed to the modal hysteretic energy demands. The contribution of the first mode reduces as the building height increases (average first mode contributions for the 3-, 9-, and 20-story frames are 95.3, 81.2, and 72.4%, respectively). Table V also shows the average and the maximum contribution from each mode for the 20-story frame for the selected set of ground motions. For the record ‘chy0809’, the second and the third modes contribute as much as 39.5 and 12.8%. Based on the average contributions from each mode, it can be concluded that for mid- to high-rise frames at least

DOI: 10.1002/eqe

Table IV. Bias factor statistics for the three buildings for roof displacement estimation.

	Bias factor (N_{MPA})					
	3-Story		9-Story		20-Story	
Ground motion record	ABSSUM	SRSS	ABSSUM	SRSS	ABSSUM	SRSS
s640r005	0.96	1.02	0.75	0.89	0.57	0.70
s503r005	0.95	0.98	0.78	0.91	0.81	0.94
s065r005	0.87	0.92	0.83	0.95	0.66	0.83
s621r004	0.95	1.00	0.80	0.94	0.66	0.83
s050r005	0.92	0.95	0.64	0.72	0.66	0.84
s212r008	0.81	0.83	0.86	1.01	0.65	0.75
s305r008	1.22	1.30	0.72	0.86	0.52	0.68
s549r009	1.10	1.16	0.82	0.96	0.64	0.77
nr	0.91	0.93	0.60	0.79	0.56	0.81
ns	0.90	0.91	0.89	1.11	0.59	0.87
chy08036	1.20	1.24	0.63	0.84	0.61	0.94
chy0809	1.17	1.20	0.52	0.66	0.55	0.92
tcu0659	1.35	1.39	0.66	0.75	0.59	0.69
syl90	1.04	1.10	0.70	0.86	0.72	0.98
newh360	0.97	1.02	0.80	1.02	0.66	0.93
nh	0.91	0.99	0.75	0.88	0.67	0.94
syl360	0.91	0.99	0.58	0.68	0.67	0.94
tcu06536	1.21	1.24	0.81	0.95	0.59	0.72
Mean	1.02	1.07	0.73	0.88	0.63	0.84
SD	0.152	0.155	0.106	0.121	0.068	0.101
CoV	0.149	0.146	0.145	0.138	0.108	0.120

the first three modes should be included in estimating the peak displacement response. This matches with the conclusions drawn in previous research works on MPA-based displacement estimation [23].

8. CONCLUSIONS

The following conclusions are drawn based on the study on the proposed method of estimation of hysteretic energy demand using multiple 'modal' equivalent systems:

- The proposed procedure provides a simple but effective means of estimating hysteretic energy demand on a structure without going through a computation-intensive nonlinear response-history analysis of the MDOF system.
- Based on the three case studies of 3-, 9-, and 20-story buildings, the proposed procedure is found to provide consistently better estimates of hysteretic energy demand than the method proposed in Ghosh and Collins' work [9].
- The proposed method is also expected to be used conveniently in energy-based design procedures since it can use energy response spectra for each ESDOF system (similar to the method proposed in [9]).

DOI: 10.1002/eqe

Table V. Mode-wise distribution of roof displacement for the 20-story building.

	D_n/D_{MPA} (where $D_{\mathrm{MPA}}=\sum_{n=1}^{5} D_n$)				
Ground motion record	Mode 1 (%)	Mode 2 (%)	Mode 3 (%)	Mode 4 (%)	Mode 5 (%)
s640r005	79.5	11.7	4.91	2.90	1.03
s503r005	85.5	9.68	3.22	1.13	0.51
s065r005	78.7	15.6	3.29	1.75	0.62
s621r004	78.3	13.8	4.95	2.02	0.96
s050r005	77.0	17.4	3.53	1.40	0.64
s212r008	85.9	10.4	2.50	0.85	0.33
s305r008	74.0	17.0	5.74	2.00	1.27
s549r009	81.7	11.8	4.40	1.44	0.65
nr	63.6	26.0	7.18	2.26	0.98
ns	60.3	28.8	7.97	2.30	0.60
chy08036	57.1	28.1	9.82	3.50	1.44
chy0809	42.7	39.5	12.8	3.73	1.38
tcu0659	85.6	11.0	2.44	0.72	0.26
syl90	70.7	18.7	6.52	3.05	1.04
newh360	66.4	22.3	7.98	2.56	0.69
nh	67.4	22.7	5.65	2.55	1.71
syl360	67.8	22.4	5.59	2.53	1.68
tcu06536	81.8	12.3	4.25	1.27	0.36
Mean	72.4	18.8	5.71	2.11	0.90
Maximum	85.9	39.5	12.8	3.73	1.71

Although the modal approach to estimating hysteretic energy looks very promising, additional studies are needed to confirm its robustness. Specifically, a larger set of earthquakes must be considered, as well as alternate building configurations. Furthermore, future research should include considerations of issues such as buildings having non-symmetrical plan, dead load and P-Delta effects, effects of strain hardening, etc.

ACKNOWLEDGEMENTS

The authors would like to thank the reviewers and the editor of this paper for their time and valuable insights and suggestions. The authors would also like to thank Amarnath Roy Chowdhury, graduate research student at IIT Bombay, for his help.

REFERENCES

1. Zahra TF, Hall WJ. Earthquake energy absorption in SDOF structures. *Journal of Structural Engineering* (ASCE) 1984; **110**(8):1757–1772.
2. Fajfar P. Equivalent ductility factors, taking into account low-cycle fatigue. *Earthquake Engineering and Structural Dynamics* 1992; **21**(10):837–848.
3. Manfredi G. Evaluation of seismic energy demand. *Earthquake Engineering and Structural Dynamics* 2001; **30**(4):485–499.
4. Housner GW. Limit design of structures to resist earthquakes. *First World Conference of Earthquake Engineering*, *Proceedings*. EERI: Berkeley, CA, U.S.A., 1956.

5. Uang C-M, Bertero VV. Use of energy as a design criterion in earthquake-resistant design. *Report No. UCB/EERC-88/18*, University of California at Berkeley, CA, U.S.A., 1998.
6. Structural Engineers Association of California (SEAOC) VISION 2000 Committee. *Performance Based Seismic Engineering of Buildings*, vol. 1. SEAOC: Sacramento, CA, U.S.A., 1995.
7. Chou C-C, Uang C-M. A procedure for evaluating seismic energy demand of framed structures. *Earthquake Engineering and Structural Dynamics* 2003; **32**(2):229–244.
8. Kunnath SK, Chai YH. Cumulative damage-based inelastic cyclic demand spectrum. *Earthquake Engineering and Structural Dynamics* 2004; **33**(4):499–520.
9. Ghosh S, Collins KR. Merging energy-based design criteria and reliability-based methods: exploring a new concept. *Earthquake Engineering and Structural Dynamics* 2006; **35**(13):1677–1698.
10. Teran-Gilmore A, Jirsa JO. Energy demands for seismic design against low-cycle fatigue. *Earthquake Engineering and Structural Dynamics* 2007; **36**(3):383–404.
11. Chopra AK, Goel RK. A modal pushover analysis procedure for estimating seismic demands for buildings. *Earthquake Engineering and Structural Dynamics* 2002; **31**(3):561–582.
12. Chopra AK, Goel RK. A modal pushover analysis procedure to estimate seismic demands for unsymmetric-plan buildings. *Earthquake Engineering and Structural Dynamics* 2004; **33**(8):903–927.
13. Ghosh S. Two alternatives for implementing performance-based seismic design of buildings—life cycle cost and seismic energy demand. *Ph.D. Thesis*, Department of Civil and Environmental Engineering, University of Michigan, Ann Arbor, MI, U.S.A., 2003.
14. International Conference of Building Officials (ICBO). *Uniform Building Code*. ICBO: Whittier, CA, U.S.A., 1997.
15. International Conference of Building Officials (ICBO). *Uniform Building Code*. ICBO: Whittier, CA, U.S.A., 1994.
16. Chou C-C. An energy-based seismic evaluation procedure for moment-resisting frames. *Ph.D. Thesis*, Department of Structural Engineering, University of California, San Diego, La Jolla, CA, U.S.A., 2001.
17. Chou C-C, Uang C-M. Evaluation of site-specific energy demand for building structures. *Seventh National Conference of Earthquake Engineering*, *Proceedings*. EERI: Boston, MA, U.S.A., 2002.
18. Gupta A, Krawinkler H. Seismic demands for performance evaluation of steel moment resisting frame structures (SAC task 5.4.3). *Report No. 132*, John A. Blume Earthquake Engineering Center, Department of Civil and Environmental Engineering, Stanford University, Stanford, CA, U.S.A., 1999.
19. Prakash V, Powell GH, Campbell S. DRAIN-2DX base program description and user guide, version 1.10. *Report No. UCB/SEMM-93/17*, University of California at Berkeley, CA, U.S.A., 1993.
20. Uzarski J, Arnold C (eds). *Earthquake Spectra*: *1999 Chi-Chi*, *Taiwan*, *Earthquake Reconnaissance Report*, Supplement A to vol. 17. EERI: Oakland, CA, U.S.A., 2001.
21. Teran-Gilmore A. On the use of spectra to establish damage control in regular frames during global predesign. *Earthquake Spectra* 2004; **20**(3):995–1020.
22. Chopra AK. *Dynamics of Structure*: *Theory and Applications to Earthquake Engineering*. Prentice-Hall: Englewood Cliffs, NJ, U.S.A., 1995.
23. Chintanapakdee C, Chopra AK. Evaluation of modal pushover analysis using generic frames. *Earthquake Engineering and Structural Dynamics* 2003; **32**(3):417–442.

DOI: 10.1002/eqe